Received: 5 September 2019 | Revised: 28 January 2020 | Accepted: 2 March 2020

DOI: 10.1002/joc.6548

RESEARCH ARTICLE

International Journal of Climatology RMetS

# Oceanic forcing of the global warming slowdown in multi-model simulations

**Xinping Xu**[1] | **Shengping He**[2] | **Tore Furevik**[2] | **Yongqi Gao**[3,4] | **Huijun Wang**[1,4,5] | **Fei Li**[2] | **Fumiaki Ogawa**[2]

[1]Collaborative Innovation Center on Forecast and Evaluation of Meteorological Disasters/Key Laboratory of Meteorological Disaster, Ministry of Education, Nanjing University of Information Science & Technology, Nanjing, China

[2]Geophysical Institute, University of Bergen and Bjerknes Centre for Climate Research, Bergen, Norway

[3]Nansen Environmental and Remote Sensing Center and Bjerknes Centre for Climate Research, Bergen, Norway

[4]Nansen-Zhu International Research Center, Institute of Atmospheric Physics, Chinese Academy of Sciences, Beijing, China

[5]Climate Change Research Center, Chinese Academy of Sciences, Beijing, China

**Correspondence**
Shengping He, Geophysical Institute, University of Bergen, Postboks 7803, 5020 Bergen, Norway.
Email: shengping.he@uib.no

**Funding information**
the CONNECTED supported by UTFORSK Partnership Program, Grant/Award Number: UTF-2016-long-term/10030; the funding of Jiangsu innovation & entrepreneurship team; the National Key R&D Program of China, Grant/Award Number: 2016YFA0600703; the National Natural Science Foundation of China, Grant/Award Numbers: 41421004, 41505073, 41605059, 41790472, 41875118; the Postgraduate Research & Practice Innovation Program of Jiangsu Province, Grant/Award Number: KYCX18_0997; the Priority Academic Program Development (PAPD) of Jiangsu Higher Education Institutions; the Young Talent Support Program by China Association for Science and Technology, Grant/Award Number: Grant 2016QNRC001

## Abstract

Concurrent with the slowdown of global warming during 2002–2013, the wintertime land surface air temperatures over Eurasia, North America, Africa, Australia, South America, and Greenland experienced notable cooling trends. The oceanic effects on the continental cooling trends are here investigated using two sets of uncoupled experiments with six different climate models. Daily and annually varying sea ice is prescribed for both sets of experiments, while daily and annually varying SST is used in the first set (EXP1) and daily and annually repeating climatological mean SST in the second set (EXP2). All six models capture the slowdown of global-mean land surface air temperature during 2002–2013 winters in EXP1 only. The slowdown concurs with a negative phase of the Pacific Decadal Oscillation (PDO), indicating that PDO plays an important role in modulating the global warming signal. Not all ensemble members capture the cooling trends over the continents, suggesting additional contribution from internal atmospheric variability.

**KEYWORDS**

continental cooling, global warming, multi-model simulations, Pacific Decadal Oscillation

## 1 | INTRODUCTION

The slowdown in the global-mean surface air temperature (GMST) trend during the beginning of the 21st century, concurring in time with a strong increase in atmospheric greenhouse gas concentrations, led to an intense public and scientific interest in the cause for the so-called global warming hiatus (Easterling & Wehner, 2009; Kosaka & Xie, 2016). Although under debate, it has been suggested that the central and eastern tropical

Pacific surface cooling played an important part in the hiatus period (1998–2012; Kosaka & Xie, 2013; Trenberth, Fasullo, Branstator, & Phillips, 2014). In boreal winter, the warming hiatus manifested as the land surface cooling and cold extremes over Northern Hemisphere mid-latitudes (Cohen, Furtado, Barlow, Alexeev, & Cherry, 2012; Johnson, Xie, Yu, & Li, 2018).

Previous studies have shown that the hiatus period was partially associated with increased stratospheric aerosol and slightly weaker solar forcing, as well as internal climate variability (Hu & Fedorov, 2017; Huber & Knutti, 2014; Kosaka & Xie, 2013; Marotzke & Forster, 2015; Meehl, Arblaster, Fasullo, Hu, & Trenberth, 2011). Using three sets of coupled model experiments, Kosaka and Xie (2013) demonstrated that tropical Pacific decadal cooling can cause unusually low GMST trend. Some other studies have also revealed results supporting such a viewpoint (England et al., 2014; Kosaka & Xie, 2016; Medhaug & Drange, 2016; Trenberth et al., 2014; Watanabe et al., 2014). For example, Trenberth et al. (2014) has simulated the global quasi-stationary wave patterns and much of the regional climate anomalies during the hiatus, by forcing an atmospheric model with an idealized heating at the equator. Deser, Guo, and Lehner (2017) found that tropical Pacific sea surface temperature (SST) and internal atmospheric variability contributed approximately equally to the GMST trend. In addition to increased heat uptake in the deeper layer of the Pacific via intensified wind-driven circulation that eventually leads to hiatus (Balmaseda, Trenberth, & Källén, 2013; England et al., 2014; Ou, Lin, & Bi, 2015; Yeo et al., 2014), heat transport to Atlantic and the southern deep oceans might have a cooling impact on the global temperature (Chen & Tung, 2014). Several studies have suggested that Arctic sea ice decline (or Arctic warming) is linked to the Eurasian winter cooling trend which might have contributed to the recent pause in global warming (Kim et al., 2014; Li, He, Li, & Wang, 2018b; Li, Wang, & Gao, 2015b; Liu, Curry, Wang, Song, & Horton, 2012; Luo et al., 2016; Mori, Watanabe, Shiogama, Inoue, & Kimoto, 2014; Outten & Esau, 2012; Wang, Chen, & Liu, 2015; Wang & Liu, 2016; Xu, He, Li, & Wang, 2018a; Xu, Li, He, & Wang, 2018b; Xu et al., 2019; Zhu, Wang, Wang, & Guo, 2018). The influence of internal atmospheric variability on the cooling of Eurasian winter climate has been inferred from Atmospheric Model Intercomparison Project (AMIP) simulations by Li, Stevens, and Marotzke (2015a).

The prominent continental cooling trends in boreal winter have aroused great research attention. The relative importance of tropical Pacific SST and radiative forcing (Kosaka & Xie, 2013), the Arctic sea ice and internal atmospheric variability (Li, Stevens, et al., 2015a), and the tropical Pacific SST and internal atmospheric variability (Deser et al., 2017), on temperature change over Eurasia, have all been examined.

In this study, the effects of SST and sea ice on the regional cooling trends on all continents (black frames in Figure 1c,d) are investigated using two sets of multi-model simulations. Six uncoupled climate models with observation-based SST and sea ice as the surface boundary are utilized. The reason why we choose uncoupled models is that the coupled models' simulations usually overestimate warming during the beginning of the 21st century (Kosaka & Xie, 2013; Medhaug, Stolpe, Fischer, & Knutti, 2017). The novelty of this study is the robust evidence from multi-model simulations which supports the oceanic effects on the global warming slowdown.

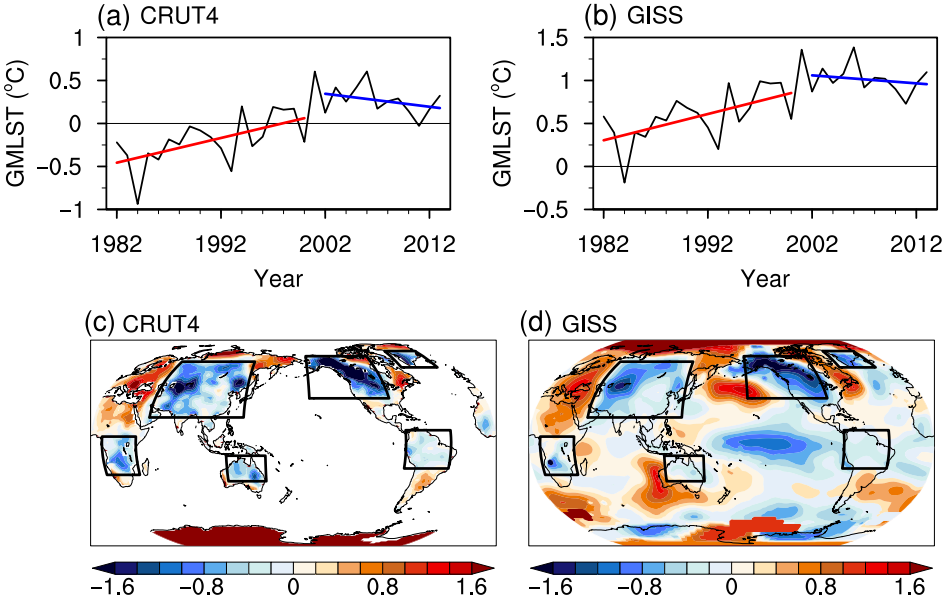


**FIGURE 1** (a) Observed GMLST anomalies (°C) in winter for 1982–2013, relative to the climatology of 1982–2013, with linear trends for 1982–2000 (red line) and 2002–2013 (blue line). (c) Observed global surface temperature trend patterns (°C·decade$^{-1}$) in winter for 2002–2013 from CRUT4. Black boxes mark the six cooling regions (Eurasia, North America, Greenland, Africa, Australia, and South America). (b, d) Same as (a, c), but from GISS, relative to the climatology of 1951–1980. CRUT4: Climate Research Unit; GISS: Goddard Institute for Space Studies [Colour figure can be viewed at wileyonlinelibrary.com]

The rest of the paper is organized as follows. Data and methods are described in section 2. The observed slowdown of continental warming is illustrated in section 3. Discussion on the simulated land surface air temperature trend in the multi-model simulations are presented in section 4. Finally, a summary is given in section 5.

## 2 | DATA AND METHODS

Datasets employed in the study include monthly surface air temperature from the Climate Research Unit, version 4 (CRUT4; https://crudata.uea.ac.uk/cru/data/hrg/; Harris, Jones, Osborn, & Lister, 2014) and Goddard Institute for Space Studies (GISS; Hansen, Ruedy, Sato, & Lo, 2010), and atmospheric variables from European Centre for Medium-Range Weather Forecasts Interim Reanalysis (ERA-I; Dee et al., 2011).

Two coordinated experiments (Ogawa et al., 2018) are performed to investigate the effects of global SST and sea ice on the climate change. Five independent uncoupled (atmosphere-only) climate models, composed of 20-member ensembles each, are adopted: CAM4 ($0.9 \times 1.25^\circ$ with 26 vertical levels up to 3 hPa; Neale et al., 2013), WACCM ($0.9 \times 1.25^\circ$ with 66 vertical levels up to 0.000006 hPa; Marsh et al., 2013), IFS (T255 with 91 vertical levels up to 0.01 hPa; Balsamo et al., 2009), IAP4 ($1.4 \times 1.4^\circ$ with 26 vertical levels up to 10 hPa; Dong, Xue, Zhang, & Zeng, 2012), and LMDZOR ($2.5 \times 1.25^\circ$ with 39 vertical levels up to 0.04 hPa; Hourdin et al., 2013). These experiments are forced by the historical forcing of CMIP5 for the years 1982–2005 and the Representative Concentration Pathway 8.5 scenarios (RCP 8.5) over 2006–2014. Daily SST and sea ice taken from NOAA OISST are used as the surface boundary forcing for the period 1982–2014 (Reynolds et al., 2007). The first set of experiment (EXP1) is forced by both daily and annually varying SST and sea ice, while the second set (EXP2) is forced by daily and annually varying sea ice but daily and annually repeating climatological mean SST (Screen, Simmonds, Deser, & Tomas, 2013). For evaluating the robustness of the results (Ogawa et al., 2018), the sixth model (AFES; $1.5 \times 1.5^\circ$ with 56 vertical levels up to 0.09 hPa; Ohfuchi et al., 2004) has the same experiment set up as the other five models, but was prescribed with monthly mean SST and sea ice from (Hurrell, Hack, Shea, Caron, & Rosinski, 2008). Thirty ensembles are performed for AFES of both experiments. No systematic deviations are found between results derived from AFES and the other five models (Koenigk et al., 2018).

The extended winter 1982 refers to November and December in 1982 and January, February, and March in 1983. The starting year of hiatus in multi-model simulations (2002) is one year later than the observed (2001) (Figure 1a,b vs. Figure 2a–f,h–m,o–t), the choice of the hiatus period (2002–2013) is therefore contrived to achieve consistency between model simulations and observations. Only land surface air temperatures are considered in this study since we focus on temperature trends over land areas and that the modelled temperatures over the oceans in the uncoupled models are nearly identical to observations. The global-mean land surface air temperature (GMLST) is calculated by area-weighted averaging.

## 3 | OBSERVED COOLING TRENDS IN MOST OF THE GLOBAL CONTINENT

Observed GMLST anomalies in winter for 1982–2013 from different datasets are provided in Figure 1. Slowdown in the rise of GMLST over 2002–2013 is striking relative to the accelerated global warming epoch 1982–2000 from the CRUT4 dataset (Figure 1a), with a transition from a warming trend that rates of approximately $0.3^\circ C \cdot decade^{-1}$ over 1982–2000 to a cooling trend in magnitude greater than $0.15^\circ C \cdot decade^{-1}$ over 2002–2013 (Figure 2g and Table 1(a)). Changes in the GISS global land temperature (Figure 1b), which is computed by removing the climatological mean from 1951 to 1980, resemble well that in the CRUT4 (Figure 1a), suggesting the robustness of the slowdown of global warming. Concurrent with the lapse in global warming reflected as dominant tropical Pacific temperature trend reduction, land surface air temperatures in most of Eurasia, North America, Africa, Australia, South America, and Greenland experience conspicuous cooling trends (Figure 1c,d). It should be noted that there is a clear pattern similar to the negative phase of the Pacific Decadal Oscillation (PDO|–; Wang & Miao, 2018) but no apparent signal of the positive phase of the Atlantic Multidecadal Oscillation (Li, Orsolini, Wang, Gao, & He, 2018a) in the surface air temperature (SAT; Figure 1d). In order to study the regional characteristics of the continental cooling trends during 2002–2013, we choose the six sub-regions (Eurasia: 50°–135°E, 20°–65°N; North America: 90°–165°W, 35°–70°N; Africa: 10°–40°E, 25°S–5°N; Australia: 120°–155°E, 30°–10°S; South America: 40°–80°W, 20°S–10°N; and Greenland: 20°–60°W, 60°–75°N) as indicated schematically by the black frames in Figure 1c,d.

Specifically, the observed regional-mean land surface air temperatures (RMLSTs) over the six sub-regions have all shown a decrease after the early 2000s (Figure 3). Note that the RMLST is defined as the ratio between the regional area-weighted averaging and the summation of

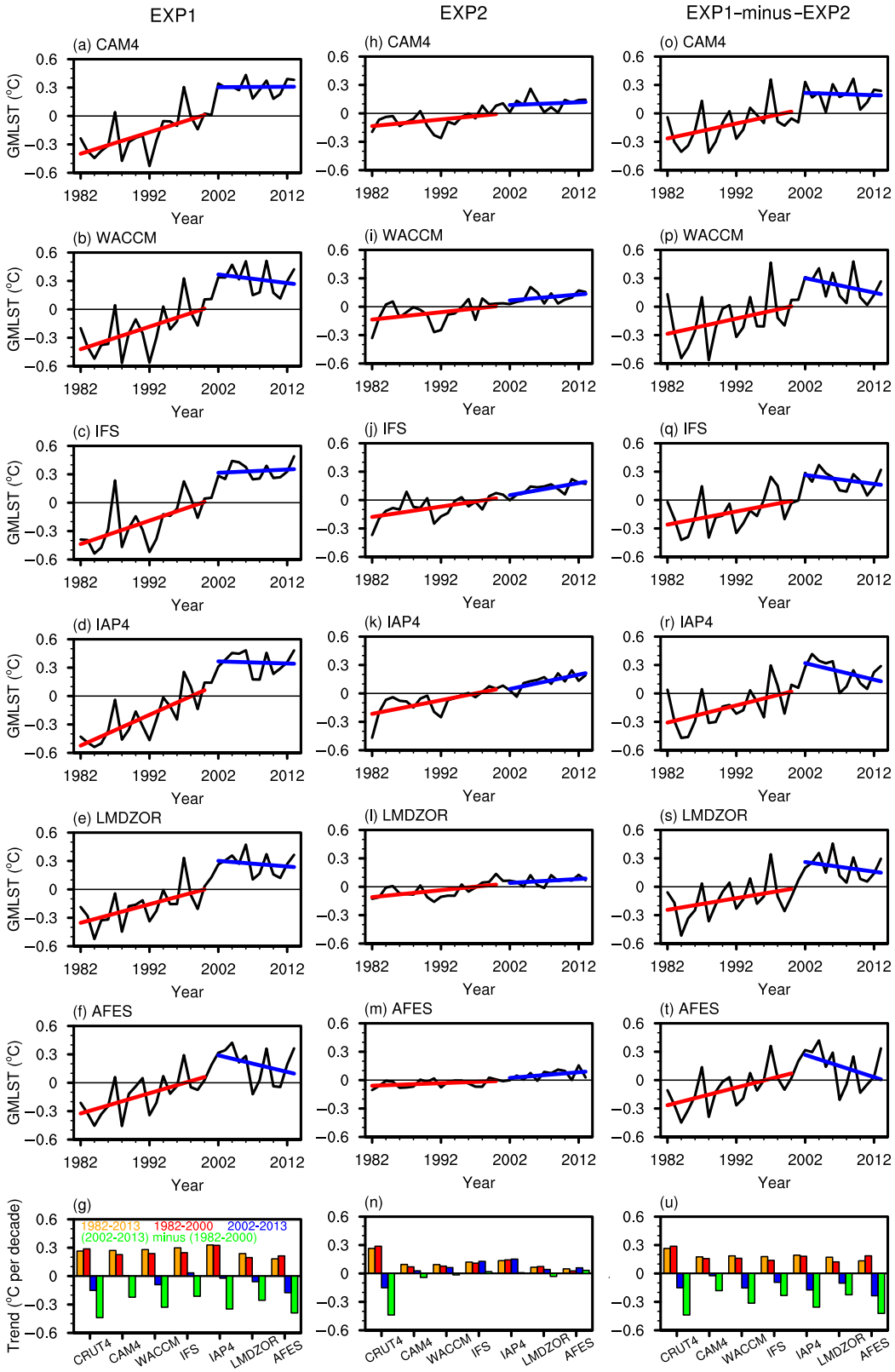


**FIGURE 2** (a–f) Simulated GMLST anomalies (°C) in winter for 1982–2013, relative to the climatology of 1982–2013, from ensembles' means of (a) CAM4, (b) WACCM, (c) IFS, (d) IAP4, (e) LMDZOR, and (f) AFES in EXP1, respectively, with linear trends for 1982–2000 (red lines) and 2002–2013 (blue lines). (g) Observed GMLST trends (°C·decade$^{-1}$) in winter from CRUT4 and simulated GMLST trends (°C·decade$^{-1}$) in winter from ensembles' means of CAM4, WACCM, IFS, IAP4, LMDZOR, and AFES in EXP1. (h–n) and (o–u) Same as (a–g), but in EXP2 and EXP1-minus-EXP2, respectively [Colour figure can be viewed at wileyonlinelibrary.com]

**TABLE 1** GMLST and RMLST trends (°C·decade$^{-1}$) in winter for 2002–2013 from CRUT4, GISS, the simulated ensembles' means of CAM4, WACCM, IFS, IAP4, LMDZOR, AFES in EXP1-minus-EXP2, respectively

| | (a) Global | (b) Eurasia | (c) North America | (d) Africa | (e) Australia | (f) South America | (g) Greenland | (h) Rest |
|---|---|---|---|---|---|---|---|---|
| CRUT4 | −0.151 | −0.125 | −0.077 | −0.027 | −0.018 | −0.017 | −0.009 | 0.121 |
| GISS | −0.089 | −0.110 | −0.086 | −0.015 | −0.005 | −0.018 | −0.007 | 0.152 |
| CAM4 | −0.024 | 0.069 | −0.073 | −0.002 | −0.024 | −0.005 | −0.008 | 0.019 |
| WACCM | −0.153 | −0.056 | −0.089 | −0.001 | −0.016 | −0.012 | −0.005 | 0.025 |
| IFS | −0.093 | 0.021 | −0.059 | 0.008 | −0.032 | −0.009 | −0.008 | −0.014 |
| IAP4 | −0.174 | −0.027 | −0.069 | −0.006 | −0.013 | −0.009 | 0.001 | −0.051 |
| LMDZOR | −0.102 | −0.040 | −0.039 | −0.004 | −0.023 | −0.009 | 0 | 0.012 |
| AFES | −0.236 | −0.018 | −0.080 | −0.006 | −0.015 | −0.021 | −0.004 | −0.092 |

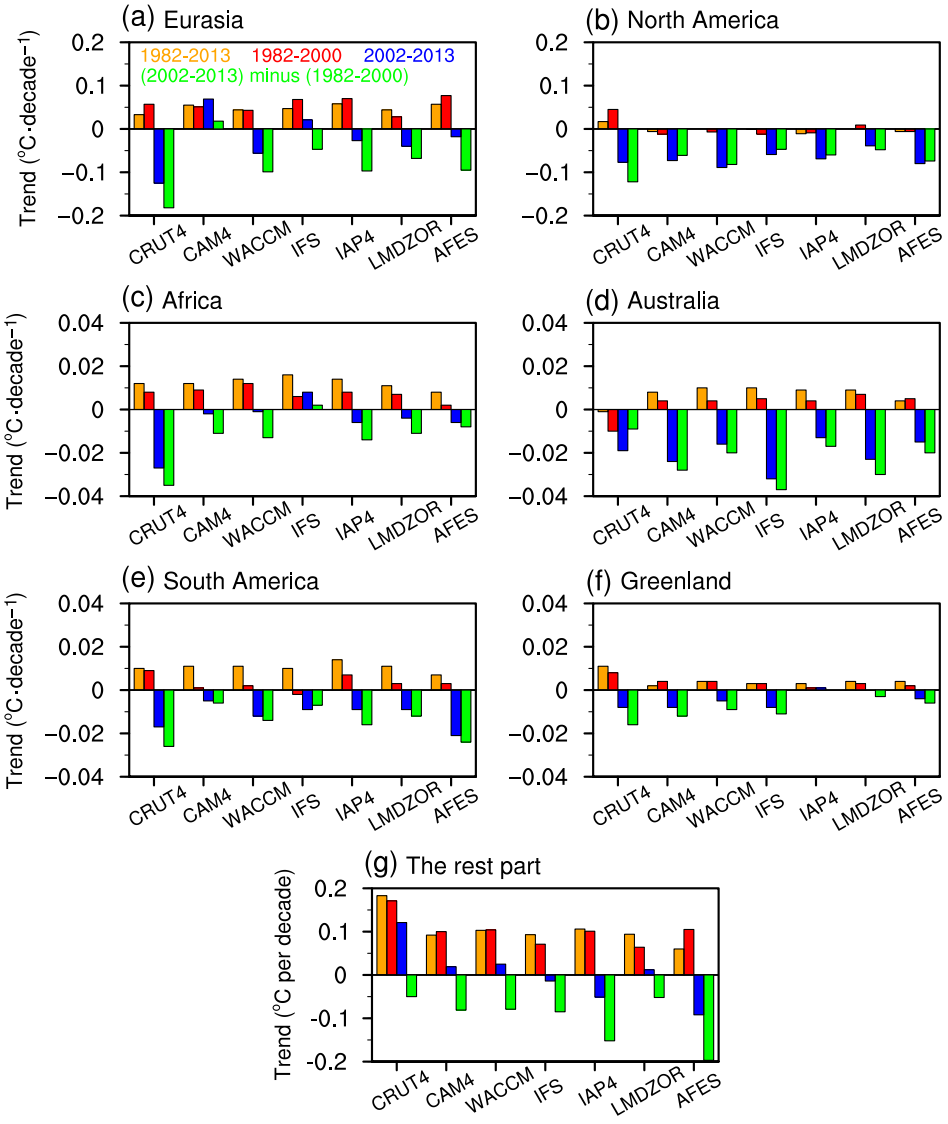


**FIGURE 3** Observed RMLST trends (°C·decade$^{-1}$) in winter from CRUT4 and simulated RMLST trends (°C·decade$^{-1}$) in winter from ensembles' means of CAM4, WACCM, IFS, IAP4, LMDZOR, and AFES in EXP1-minus-EXP2 over (a) Eurasia, (b) North America, (c) Africa, (d) Australia, (e) South America, (f) Greenland, and (g) the rest part of the globe, respectively [Colour figure can be viewed at wileyonlinelibrary.com]

global land grids, in order to quantitatively present the regional contributions to the GMLST trend. Eurasia shows the strongest slowdown in surface warming; for instance, the Eurasian temperature trend reverses from a warming of 0.057°C·decade$^{-1}$ over 1982–2000 to a cooling of −0.125°C·decade$^{-1}$ over 2002–2013 (Figure 3a and

Tables 1(b) vs. 2(b)). North America comes in the second with a RMLST trend of −0.077°C·decade$^{-1}$ for 2002–2013, reduced by 0.122°C·decade$^{-1}$ compared to the previous warming period (Figure 3b and Tables 1(c) vs. 2(c)). For the other four sub-regions, RMLST trends in the latter period are −0.027°C·decade$^{-1}$ over Africa, −0.018°C·decade$^{-1}$ over Australia, −0.017°C·decade$^{-1}$ over South America, and −0.009°C·decade$^{-1}$ over Greenland, respectively (Figure 3c–f and Table 1(d)–(g)). Covering relatively small land areas compared to the global land, winter surface temperatures in these regions all make a cooling contribution to the GMLST trend (−0.151°C·decade$^{-1}$).

## 4 | RESULTS FROM MULTI-MODEL SIMULATIONS

We first address whether the six models can reproduce the realistic GMLST variability. During 1982–2013, the correlations between the observed GMLST and the simulated GMLST in the ensemble-mean of CAM4, WACCM, IFS, IAP4, LMDZOR, and AFES simulations in the EXP1 range from 0.77 to 0.84 (significant at 99% confidence level; Table 3(a)). In the EXP2, the linear correlations with observations are lower than those in the EXP1 but still significant at 99% confidence level (Table 3(a)). The simulated GMLST in the EXP1 is also closer to the observed GMLST in magnitude than that in the EXP2 (Figure 2a–f vs. h–m). Although the simulations suggest the contribution of both SST and sea ice to the GMLST, it is interesting to note that global SST and sea ice variations jointly account for 59.3–70.6% of the inter-annual variability of GMLST, approximately double of that explained by sea ice alone (Table 3(b)). As shown in Figure 2g,n, EXP1 reproduces the slowdown of warming trend in the GMLST which has not been reproduced by the EXP2. The oceanic effect is further estimated through subtracting the simulations in the EXP2 from EXP1 (referred to as EXP1-minus-EXP2; Screen, Deser, & Simmonds, 2012). As shown in Figure 2o–t, EXP1-minus-EXP2 effectively depicts the time evolution of the observed GMLST, with the highest correlation coefficient of 0.80 (Table 3(a)). The impact of global SST, indicated by the EXP1-minus-EXP2, can explain 46.2–64.0% of the GMLST variance (Table 3(b)). More specifically, global SST changes have lowered the fully forced GMLST trend

**TABLE 2** Same as Table 1, but for 1982–2000

| | (a) Global | (b) Eurasia | (c) North America | (d) Africa | (e) Australia | (f) South America | (g) Greenland | (h) Rest |
|---|---|---|---|---|---|---|---|---|
| CRUT4 | 0.288 | 0.057 | 0.045 | 0.009 | −0.010 | 0.009 | 0.009 | 0.171 |
| GISS | 0.306 | 0.087 | 0.040 | 0.000 | −0.007 | 0.010 | 0.008 | 0.167 |
| CAM4 | 0.157 | 0.051 | −0.012 | 0.009 | 0.004 | 0.001 | 0.004 | 0.100 |
| WACCM | 0.161 | 0.043 | −0.007 | 0.012 | 0.004 | 0.002 | 0.004 | 0.104 |
| IFS | 0.139 | 0.068 | −0.012 | 0.006 | 0.006 | −0.002 | 0.003 | 0.071 |
| IAP4 | 0.182 | 0.070 | −0.009 | 0.008 | 0.004 | 0.007 | 0.001 | 0.101 |
| LMDZOR | 0.122 | 0.028 | 0.009 | 0.007 | 0.007 | 0.003 | 0.003 | 0.064 |
| AFES | 0.187 | 0.077 | −0.006 | 0.002 | 0.005 | 0.003 | 0.002 | 0.105 |

**TABLE 3** Correlation coefficients between GMLST anomalies from CRUT4 and the simulated ensembles' means of CAM4, WACCM, IFS, IAP4, LMDZOR, and AFES in EXP1, EXP2, and EXP1-minus-EXP2, respectively, and the corresponding variance that explained by natural forcing

| | (a) Correlation coefficient | | | (b) Explained variance (%) | | |
|---|---|---|---|---|---|---|
| | EXP1 | EXP2 | EXP1-minus-EXP2 | EXP1 | EXP2 | EXP1-minus-EXP2 |
| CAM4 | 0.77 | 0.61 | 0.68 | 59.3 | 37.2 | 46.2 |
| WACCM | 0.81 | 0.48 | 0.74 | 65.6 | 23.0 | 54.8 |
| IFS | 0.78 | 0.60 | 0.75 | 60.8 | 36.0 | 56.3 |
| IAP4 | 0.81 | 0.56 | 0.78 | 68.4 | 31.4 | 60.8 |
| LMDZOR | 0.84 | 0.51 | 0.80 | 70.6 | 26.0 | 64.0 |
| AFES | 0.80 | 0.45 | 0.75 | 64.0 | 20.3 | 56.3 |

in the six models to −0.024, −0.153, −0.093, −0.174, −0.102, and −0.236°C·decade$^{-1}$, respectively, close to the observed trend of −0.151°C·decade$^{-1}$ (Figure 2u and Table 1(a)). The successful simulation of inter-annual variability and recent warming slowdown of the GMLST by most of the models implies the potential influence of global SST and sea ice on the global continental temperature variability, with SST being the dominant factor.

Regionally, cooling trends over North America, Africa, Australia, and South America are generally reproduced by the EXP1 and EXP1-minus-EXP2 (Figures 3a–f and 4a–f,m–r). While the simulated

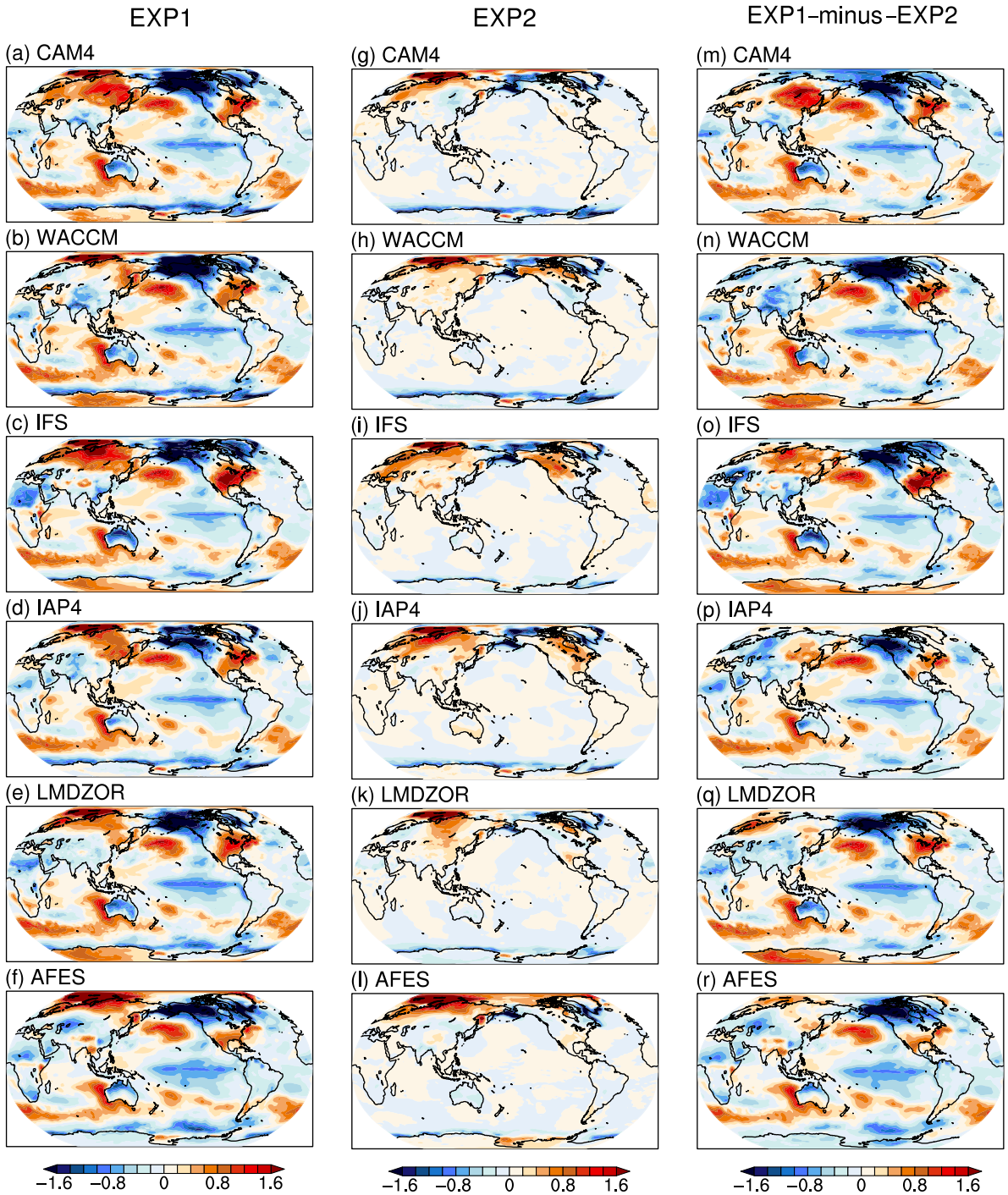


**FIGURE 4** (a–f) Simulated global surface temperature trend patterns (°C·decade$^{-1}$) in winter for 2002–2013 from ensembles' means of (a) CAM4, (b) WACCM, (c) IFS, (d) IAP4, (e) LMDZOR, and (f) AFES in EXP1, respectively. (g–l) and (m–r) same as (a–f), but in EXP2 and EXP1-minus-EXP2, respectively [Colour figure can be viewed at wileyonlinelibrary.com]

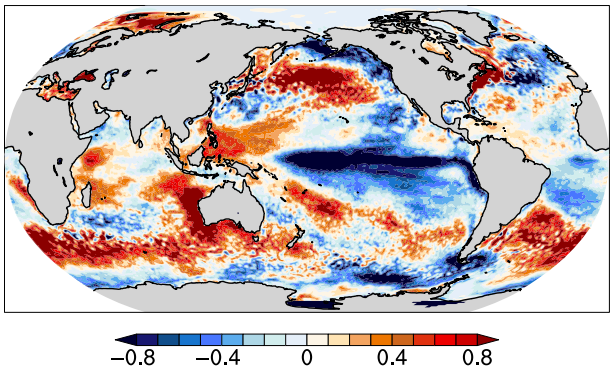


**FIGURE 5** Global SST trend patterns (°C·decade$^{-1}$) in winter for 2002–2013 from EXP1 [Colour figure can be viewed at wileyonlinelibrary.com]

Eurasian winter temperature trend shows diversity among models. WACCM, IAP4, LMDZOR, and AFES ensembles show a slight cooling of the Eurasian winter climate, but CAM4 and IFS capture a slight warming trend in the high latitudes of Eurasia (Figures 3a and 4m–r). The EXP1-minus-EXP2 displays broadly similar trend patterns with the EXP1, except for the absent warming over the Barents–Kara Seas (Figure 4a–f vs. m–r). It can be seen that the spatial distribution of the forced tropical cooling and extratropical warming over the Pacific Ocean resemble the PDO|−, accompanied with weak cooling trends above the North Atlantic Ocean (Figure 4m–r). Moreover, the PDO|− signal is the most dominant feature in the trend of the daily varying global SST which is prescribed as one of the boundaries in the EXP1 (Figure 5). The presence of the PDO|− in both the SAT and SST trend fields indicates the atmospheric response to SST variability in numerical simulations and thus suggests the potential influence of the PDO|− on the slowdown of warming trend in the GMLST, consistent with a previous numerical study (Trenberth et al., 2014). Also, the PDO|− pattern is complemented with strong easterly winds in the tropical Pacific and remarkable change of the sea level pressure in the subtropics in both reanalysis (Figure 6a) and numerical simulations (Figure 6b–g). The observed upper tropospheric global teleconnection wave patterns from the tropics to extratropics (Figure 6h) are proposed as possible mechanisms through which the PDO|− causes regional climate anomalies during the hiatus (Trenberth et al., 2014). Here, the wave trains have also been generally replicated (Figure 6i–n), supporting the hypothesis that the PDO|− could lead to continental cooling.

It is worth noting that the model ensemble mean reduces the amplitude of internal variability relative to prescribed forcing (Ogawa et al., 2018). A recent study by Sung et al. (2019) emphasized the role of internal climate variability on the remarkable North American cooling. In addition to the fundamental effect of PDO (Sung, Kim, Baek, Lim, & Kim, 2016), we further examine the potential role of atmospheric internal dynamics through removing the ensemble mean of each model from individual members in the EXP1. It shows that six members from CAM4, six members from WACCM, three members from IFS, seven members from IAP4, six members from LMDZOR, and ten members from AFES (from which the ensemble mean has been removed) did reproduce the North American cooling trend (identified by the threshold above 0.5°C·decade$^{-1}$ over North America), though the temperature trend over the ocean becomes considerably weak (Figure 7a–f). The accompanied intensification of the anticyclonic ridge near Alaska and cyclone to the south (Figure 8a–f), which show a basin-scale north–south atmospheric circulation over the North Pacific, resemble the negative phase of the North Pacific Oscillation (NPO|−; Lee, Hong, & Hsu, 2015; Rogers, 1981). The overlying atmospheric circulation trend in the upper troposphere (Figure 8g–l) corresponds to the negative phase of the Pacific North America (PNA|−) pattern (Wallace & Gutzler, 1981). It suggests that the internal atmospheric variability might also be a possible driver for the North American cooling (Sung et al., 2019). Therefore, our results suggest that the internal atmospheric variability still has impacts on climate change though the contribution of external forcing is dominant.

Apparent temperature trends mainly occur in high latitudes of Northern Hemisphere in the EXP2, showing much weaker amplitude over North America relative to EXP1-minus-EXP2 (Figure 4g–l vs. m–r). Strong warming emerges over the Barents–Kara Seas and subarctic Russia, while the observed surface warming in the East Siberian–Chukchi Seas, which is suggested to be responsible for North American cold winters (Kug et al., 2015), is not clear in the EXP2 (Figure 4g–l). The feature of Eurasian temperature trend in the multi-model simulations forced by sea ice variations is also interesting. Generally, cooling in two (Figure 4g,l) and warming in four (Figure 4h–k) sets of simulations over Eurasia make it difficult to attribute the Eurasian cooling to the reduction of sea ice in this study. A recent study by Ogawa et al. (2018), which is based on the same model simulations, has focused on the impacts of Arctic sea ice loss on the Eurasian winter cooling trend. Only a small number of members in both experiments can simulate Eurasian cooling trend with the observed amplitude (Ogawa et al., 2018, fig. 3), leading to the conclusion that atmospheric internal dynamics instead of sea ice changes might play an important role in the observed Eurasian cooling. In this study, some individual members of EXP1, from which the ensemble mean has been removed, have

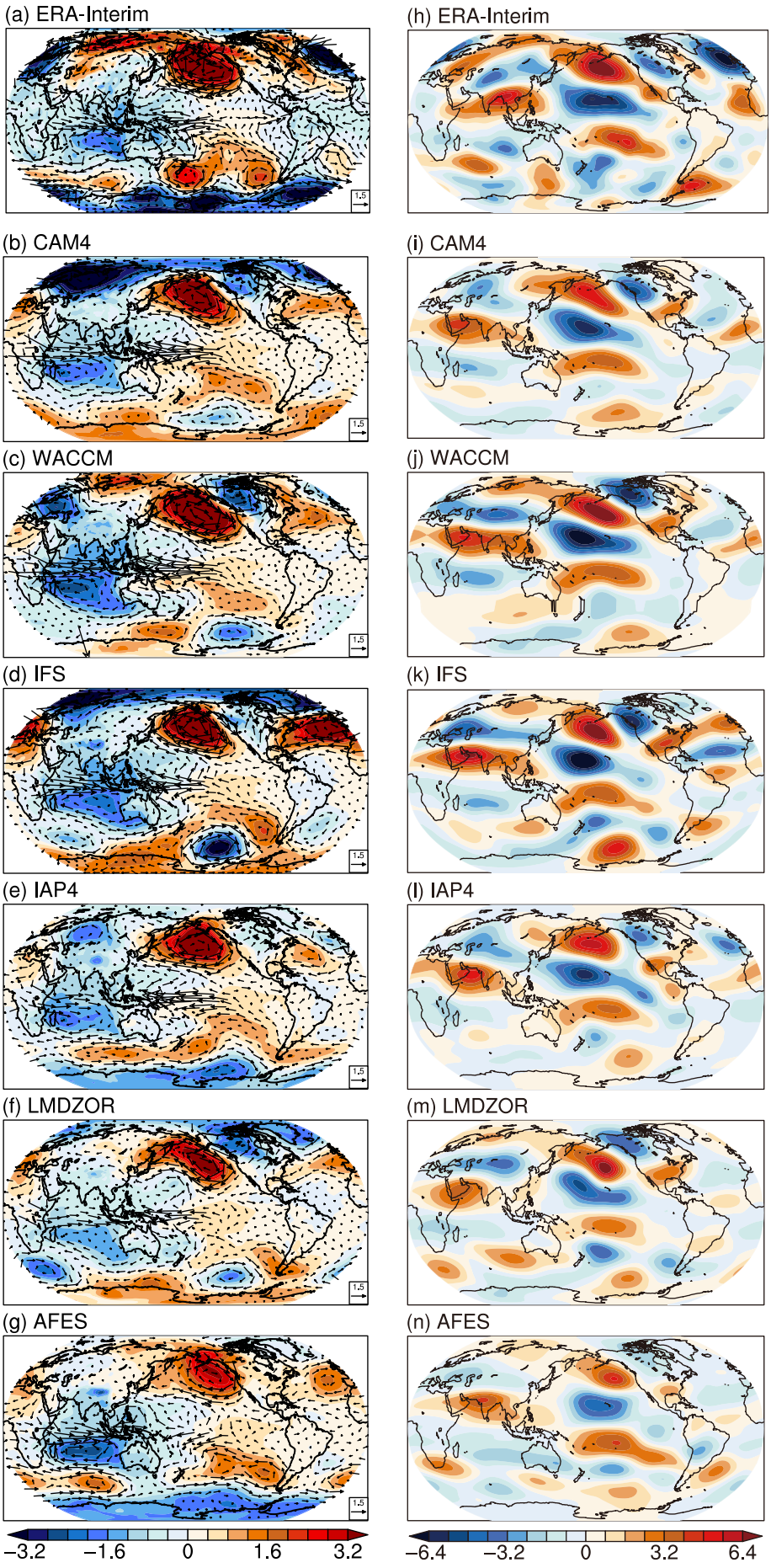


**FIGURE 6** (a) Sea level pressure (shading) and 850-hPa vector winds (vectors) and (h) 300-hPa streamfunction trend patterns ($10^6$ $m^2 \cdot s^{-1} \cdot decade^{-1}$) in winter for 2002–2013 from ERA-I. (b–g) Same as (a), (i–n) same as (h), but for simulated ones from ensembles' means of (b, i) CAM4, (c, j) WACCM, (d, k) IFS, (e, l) IAP4, (f, m) LMDZOR, and (g, n) AFES in EXP1-minus-EXP2, respectively. ERA-I: European Centre for Medium-Range Weather Forecasts Reanalysis ERA-Interim [Colour figure can be viewed at wileyonlinelibrary.com]

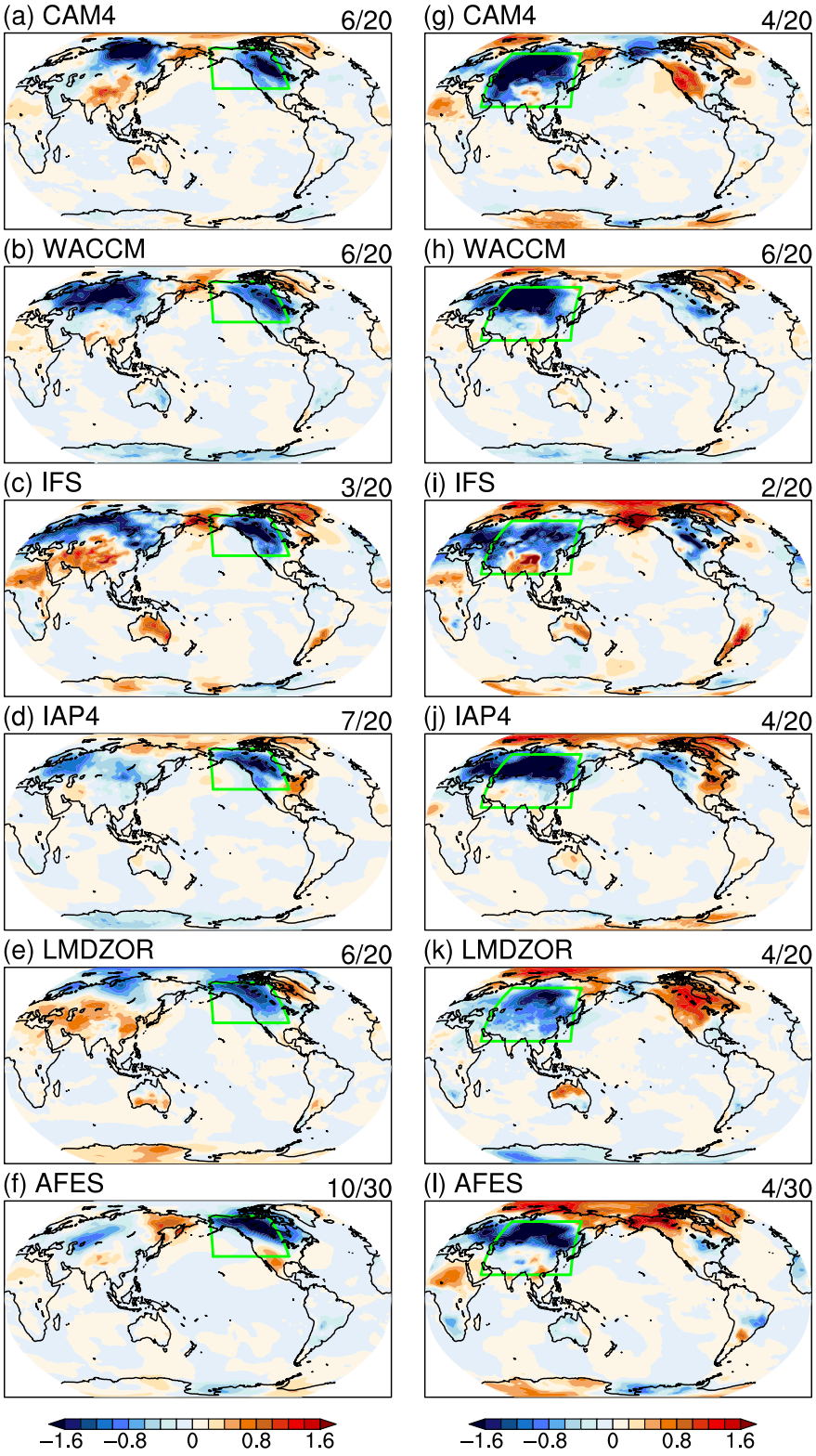


**FIGURE 7** Simulated global surface temperature trend patterns (°C·decade$^{-1}$) in winter for 2002–2013 from the ensemble members (from which the model ensemble mean has been removed) that have simulated the North American cooling trend in (a) CAM4, (b) WACCM, (c) IFS, (d) IAP4, (e) LMDZOR, and (f) AFES in EXP1, respectively. (g–l) Same as (a–f), but for ensemble members that have simulated the Eurasian cooling trend [Colour figure can be viewed at wileyonlinelibrary.com]

captured the cooling trend in Eurasia and warming trend in the Barents–Kara Seas (Figure 7g–l). Correspondingly, an intensified surface high pressure over Northern Eurasia (Honda, Inoue, & Yamane, 2009) is found in these individual members (Figure 8m–r), consistent with the reanalysis (Figure 5a). High-latitude internal variability (Figure 8m–x) thus seems to play a role in the process. On the other hand, some other modelling studies suggest that Arctic sea ice loss can result in Eurasian cooling (Kim et al., 2014; Liu et al., 2012; Mori et al., 2014). Mori,

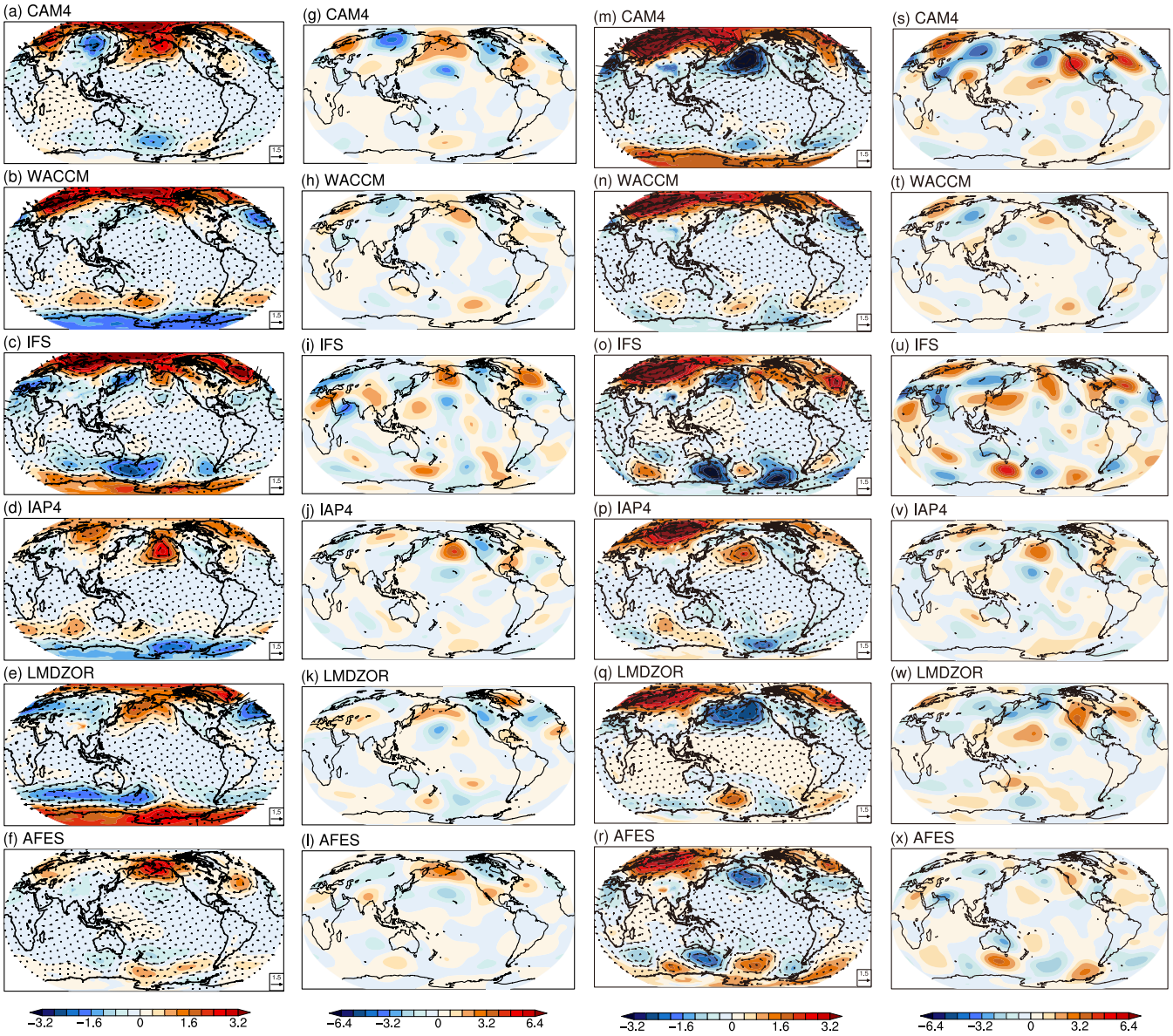


**FIGURE 8** (a–f) Simulated sea level pressure (shading) and 850-hPa vector winds (vectors) and (g–l) 300-hPa streamfunction trend patterns ($10^6$ $m^2 \cdot s^{-1} \cdot decade^{-1}$) in winter for 2002–2013 from the ensemble members (from which the model ensemble mean has been removed) that have simulated the North American cooling trend in (a, g) CAM4, (b, h) WACCM, (c, i) IFS, (d, j) IAP4, (e, k) LMDZOR, and (f, l) AFES in EXP1, respectively. (m–x) Same as (a–l), but for the ensemble members that have simulated the Eurasian cooling trend [Colour figure can be viewed at wileyonlinelibrary.com]

Kosaka, Watanabe, Nakamura, and Kimoto (2019) concluded that ~44% of the Eurasian cooling trend in recent decades is due to sea ice loss in the Barents–Kara Seas by using a hybrid analysis of observations and multi-model ensembles from atmospheric general circulation models. Both viewpoints can get supporting evidences from our multi-model simulations (Figures 4 and 7), which explains why it has been a controversial issue whether the Arctic sea ice loss (Kim et al., 2014; Liu et al., 2012; Mori et al., 2014, 2019) or internal atmospheric variability (Kosaka & Xie, 2013; Li, Stevens, et al., 2015a; McCusker, Fyfe, & Sigmond, 2016; Ogawa et al., 2018; Sun, Perlwitz, & Hoerling, 2016) can influence Eurasian winter climate.

Quantitatively, RMLST trends simulated by the EXP1-minus-EXP2 are in broad agreement with the observations, except for those over Eurasia (Figure 3). In response to the oceanic forcing, the simulated RMLST in North America exhibits a cooling trend of −0.073, −0.089, −0.059, −0.069, −0.039, and −0.080°C·decade$^{-1}$ during 2002–2013, approximate to the observed −0.077°C·decade$^{-1}$ (Figure 3b and Table 1(c)). Over the

other four sub-regions, the simulated RMLST trends are close to the observed ones (Figure 3c–f and Table 1(d)–(g)). Note that the observed Greenland cooling is not well reproduced by two models in the EXP1-minus-EXP2 (Figures 3f and 4p–q), which is likely associated with the atmospheric teleconnection (e.g., the North Atlantic Oscillation; figure not shown) as suggested by previous studies (Hurrell, 1995; Hurrell, Kushnir, & Visbeck, 2001). In general, the high consistency between the RMLST trends in observations and numerical simulations (Figure 3), which targets potentially the response to dominate SST change, strengthens the hypothesis that the PDO|− largely explains the surface temperature cooling trends contributing to the slowdown of warming trend in GMLST.

The comparisons of atmospheric response between simulations forced with observed daily-varying SST and daily-varying sea ice and those forced with climatological SST and daily-varying sea ice have suggested the potential oceanic contribution to the slowdown of global warming. The results are consistent with previous studies (such as Kosaka & Xie, 2013). However, it might be noted that the effects of SST and sea ice have not been totally separated in this study due to the potential interaction between SST and sea ice. Further study can focus on the atmospheric response to the observed daily-varying SST and climatological sea ice, which will further improve our understanding of oceanic impacts on climate. Additionally, the simulations in this study are not suitable to investigate the role of external forcing on the continental cooling, which, however, has been revealed by many studies (Fyfe, von Salzen, Cole, Gillett, & Vernier, 2013; Huber & Knutti, 2014; Marotzke & Forster, 2015; Santer et al., 2014). For example, a modelling study of Fyfe et al. (2013) suggested that increasing stratospheric aerosol since the late 1990s has a global cooling impact of about 0.07°C·decade$^{-1}$. Such knowledge on the global warming slowdown will improve our understanding of climate change in the future.

## 5 | SUMMARY

Observations indicate that the land surface air temperatures over Eurasia, North America, Africa, Australia, South America, and Greenland exhibit remarkable cooling trends, concurrent with the slowdown of global warming during 2002–2013. The regional-mean land surface air temperatures (RMLSTs) over the six sub-regions have shown cooling trend with rate of −0.125, −0.077, −0.027, −0.018, −0.017, and −0.009°C·decade$^{-1}$ during 2002–2013, contributing to the global-mean land surface temperature (GMLST) cooling trend of −0.151°C·decade$^{-1}$.

The inter-annual variability and recent warming slowdown of GMLST are successfully reproduced by the multi-model simulations. Global SST and sea ice anomalies in combination play a major role, and that oceanic contribution dominates. The observed global teleconnection wave trains, which are suggested associated with the PDO|−, have been reproduced by the multi-model simulations. We thus hypothesize that the wintertime cooling trends in North America, Africa, Australia, South America, and Greenland during 2002–2013 might be the response to the shift of the PDO to its negative phase. Additionally, the internal atmospheric variability has also contributed to the cooling trend over Eurasia and North American. It might be noted that there is an apparent La Niña-like decadal cooling trend which may also contribute to the global warming hiatus. However, the multi-model simulations in the present study cannot identify the impact of regional SST. Further investigation is needed in this regard, and numerical simulation by multi-models is an essential way to understand the climate response to the natural forcing.

## ACKNOWLEDGEMENTS

This research was supported by the National Key R&D Program of China (2016YFA0600703), the CONNECTED supported by UTFORSK Partnership Program (UTF-2016-long-term/10030), the National Natural Science Foundation of China (Grants 41875118, 41505073, 41605059, 41421004, and 41790472), the Young Talent Support Program by China Association for Science and Technology (Grant 2016QNRC001), the Postgraduate Research & Practice Innovation Program of Jiangsu Province (KYCX18_0997), the funding of Jiangsu innovation & entrepreneurship team, and the Priority Academic Program Development (PAPD) of Jiangsu Higher Education Institutions.

## CONFLICT OF INTEREST

The authors declare no potential conflict of interest.

## ORCID

*Xinping Xu* https://orcid.org/0000-0002-5116-5169
*Shengping He* https://orcid.org/0000-0003-4245-357X

## REFERENCES

Balmaseda, M.A., Trenberth, K.E. and Källén, E. (2013) Distinctive climate signals in reanalysis of global ocean heat content. *Geophysical Research Letters*, 40, 1754–1759.

Balsamo, G., Viterbo, P., Beljaars, A., Hurk, B.V.D., Hirschi, M., Betts, A.K. and Scipal, K. (2009) A revised hydrology for the ECMWF model: Verification from field site to terrestrial water storage and impact in the Integrated Forecast System. *Journal of Hydrometeorology*, 10, 623–643.

Chen, X. and Tung, K.-K. (2014) Varying planetary heat sink led to global-warming slowdown and acceleration. *Science*, 345, 897.

Cohen, J.L., Furtado, J.C., Barlow, M., Alexeev, V.A. and Cherry, J. E. (2012) Asymmetric seasonal temperature trends. *Geophysical Research Letters*, 39, L04705.

Dee, D.P., Uppala, S.M., Simmons, A.J., Berrisford, P., Poli, P., Kobayashi, S., Andrae, U., Balmaseda, M.A., Balsamo, G. and Bauer, P. (2011) The ERA-Interim reanalysis: Configuration and performance of the data assimilation system. *Quarterly Journal of the Royal Meteorological Society*, 137, 553–597.

Deser, C., Guo, R. and Lehner, F. (2017) The relative contributions of tropical Pacific sea surface temperatures and atmospheric internal variability to the recent global warming hiatus. *Geophysical Research Letters*, 44,7945–7954. https://doi.org/10.1002/2017GL074273.

Dong, X., Xue, F., Zhang, H. and Zeng, Q. (2012) Evaluation of surface air temperature change over China and the globe during the twentieth century in IAP AGCM4.0. *Atmospheric and Oceanic Science Letters*, 5, 435–438.

Easterling, D.R. and Wehner, M.F. (2009) Is the climate warming or cooling? *Geophysical Research Letters*, 36, 262–275.

England, M.H., Mcgregor, S., Spence, P., Meehl, G.A., Timmermann, A., Cai, W., Gupta, A.S., Mcphaden, M.J., Purich, A. and Santoso, A. (2014) Recent intensification of wind-driven circulation in the Pacific and the ongoing warming hiatus. *Nature Climate Change*, 4, 222–227.

Fyfe, J.C., von Salzen, K., Cole, J.N.S., Gillett, N.P. and Vernier, J.P. (2013) Surface response to stratospheric aerosol changes in a coupled atmosphere-ocean model. *Geophysical Research Letters*, 40, 584–588.

Hansen, J., Ruedy, R., Sato, M. and Lo, K. (2010) Global surface temperature change. *Reviews of Geophysics*, 48, RG4004.

Harris, I., Jones, P.D., Osborn, T.J. and Lister, D. (2014) Updated high-resolution grids of monthly climatic observations—The CRU TS3.10 dataset. *International Journal of Climatology*, 34, 623–642.

Honda, M., Inoue, J. and Yamane, S. (2009) Influence of low Arctic sea-ice minima on anomalously cold Eurasian winters. *Geophysical Research Letters*, 36, L08707.

Hourdin, F., Foujols, M.A., Codron, F., Guemas, V., Dufresne, J.L., Bony, S., Denvil, S., Guez, L., Lott, F., Ghattas, J., Braconnot, P., Marti, O., Meurdesoif, O. and Bopp, L. (2013) Impact of the LMDZ atmospheric grid configuration on the climate and sensitivity of the IPSL-CM5A coupled model. *Climate Dynamics*, 40, 2167–2192.

Hu, S. and Fedorov, A.V. (2017) The extreme El Niño of 2015–2016 and the end of global warming hiatus. *Geophysical Research Letters*, 44, 3816–3824.

Huber, M. and Knutti, R. (2014) Natural variability, radiative forcing and climate response in the recent hiatus reconciled. *Nature Geoscience*, 7, 651–656.

Hurrell, J.W. (1995) Decadal trends in the North Atlantic Oscillation region temperatures and precipitation. *Science*, 269, 676–679.

Hurrell, J.W., Hack, J.J., Shea, D., Caron, J.M. and Rosinski, J. (2008) A new sea surface temperature and sea ice boundary dataset for the Community Atmosphere Model. *Journal of Climate*, 21, 5145–5153.

Hurrell, J.W., Kushnir, Y. and Visbeck, M. (2001) The North Atlantic Oscillation. *Science*, 291, 603–605.

Johnson, N.C., Xie, S.-P., Yu, K. and Li, X. (2018) Increasing occurrence of cold and warm extremes during the recent global warming slowdown. *Nature Communications*, 9, 1724.

Kim, B.M., Son, S.W., Min, S.K., Jeong, J.H., Kim, S.J., Zhang, X., Shim, T. and Yoon, J.H. (2014) Weakening of the stratospheric polar vortex by Arctic sea-ice loss. *Nature Communications*, 5, 4646.

Koenigk, T., Gao, Y., Gastineau, G., Keenlyside, N., Nakamura, T., Ogawa, F., Orsolini, Y., Semenov, V., Suo, L., Tian, T., Wettstein, J.J. and Yang, S. (2018) Impact of Arctic sea ice variations on winter temperature anomalies in northern hemispheric land areas. *Climate Dynamics*, 52, 3111–3137.

Kosaka, Y. and Xie, S.-P. (2013) Recent global-warming hiatus tied to equatorial Pacific surface cooling. *Nature*, 501, 403–407.

Kosaka, Y. and Xie, S.-P. (2016) The tropical Pacific as a key pacemaker of the variable rates of global warming. *Nature Geoscience*, 9, 669–673.

Kug, J.S., Jeong, J.H., Jang, Y.S., Kim, B.M., Folland, C.K., Min, S. K. and Son, S.W. (2015) Two distinct influences of Arctic warming on cold winters over North America and East Asia. *Nature Geoscience*, 8, 759–762.

Lee, M.Y., Hong, C.C. and Hsu, H.H. (2015) Compounding effects of warm sea surface temperature and reduced sea ice on the extreme circulation over the extratropical North Pacific and North America during the 2013–2014 boreal winter. *Geophysical Research Letters*, 42, 1612–1618.

Li, C., Stevens, B. and Marotzke, J. (2015a) Eurasian winter cooling in the warming hiatus of 1998–2012. *Geophysical Research Letters*, 42, 8131–8139.

Li, F., Orsolini, Y.J., Wang, H., Gao, Y. and He, S. (2018a) Atlantic Multidecadal Oscillation modulates the impacts of Arctic sea ice decline. *Geophysical Research Letters*, 45, 2497–2506. https://doi.org/10.1002/2017GL076210.

Li, F., Wang, H. and Gao, Y. (2015b) Change in sea ice cover is responsible for non-uniform variation in winter temperature over East Asia. *Atmospheric and Oceanic Science Letters*, 8, 376–382.

Li, S., He, S., Li, F. and Wang, H. (2018b) Simulated and projected relationship between the East Asian winter monsoon and winter Arctic Oscillation in CMIP5 models. *Atmospheric and Oceanic Science Letters*, 11, 417–424.

Liu, J., Curry, J.A., Wang, H., Song, M. and Horton, R.M. (2012) Impact of declining Arctic sea ice on winter snowfall. *Proceedings of the National Academy of Sciences of the United States of America*, 109, 4074–4079.

Luo, D., Xiao, Y., Yao, Y., Dai, A., Simmonds, I. and Franzke, C.L. E. (2016) Impact of Ural blocking on winter warm Arctic-cold Eurasian anomalies. Part I: Blocking-induced amplification. *Journal of Climate*, 29, 3925–3947.

McCusker, K.E., Fyfe, J.C. and Sigmond, M. (2016) Twenty-five winters of unexpected Eurasian cooling unlikely due to Arctic sea-ice loss. *Nature Geoscience*, 9, 838–842.

Marotzke, J. and Forster, P.M. (2015) Forcing, feedback and internal variability in global temperature trends. *Nature*, 517, 565–570.

Marsh, D.R., Mills, M.J., Kinnison, D.E., Lamarque, J.F., Calvo, N. and Polvani, L.M. (2013) Climate change from 1850 to 2005 simulated in CESM1(WACCM). *Journal of Climate*, 26, 7372–7391.

Medhaug, I. and Drange, H. (2016) Global and regional surface cooling in a warming climate: A multi-model analysis. *Climate Dynamics*, 46, 3899–3920.

Medhaug, I., Stolpe, M.B., Fischer, E.M. and Knutti, R. (2017) Reconciling controversies about the "global warming hiatus". *Nature*, 545, 41–47.

Meehl, G.A., Arblaster, J.M., Fasullo, J.T., Hu, A. and Trenberth, K. E. (2011) Model-based evidence of deep-ocean heat uptake during surface-temperature hiatus periods. *Nature Climate Change*, 1, 360–364.

Mori, M., Kosaka, Y., Watanabe, M., Nakamura, H. and Kimoto, M. (2019) A reconciled estimate of the influence of Arctic sea-ice loss on recent Eurasian cooling. *Nature Climate Change*, 9, 123–129.

Mori, M., Watanabe, M., Shiogama, H., Inoue, J. and Kimoto, M. (2014) Robust Arctic sea-ice influence on the frequent Eurasian cold winters in past decades. *Nature Geoscience*, 7, 869–873.

Neale, R.B., Richter, J., Park, S., Lauritzen, P.H., Vavrus, S.J., Rasch, P.J. and Zhang, M. (2013) The mean climate of the Community Atmosphere Model (CAM4) in forced SST and fully coupled experiments. *Journal of Climate*, 26, 5150–5168.

Ogawa, F., Keenlyside, N., Gao, Y., Koenigk, T., Yang, S., Suo, L., Wang, T., Gastineau, G., Nakamura, T., Cheung, H.N., Omrani, N.-E., Ukita, J. and Semenov, V. (2018) Evaluating impacts of recent Arctic sea ice loss on the Northern Hemisphere winter climate change. *Geophysical Research Letters*, 45, 3255–3263. https://doi.org/10.1002/2017GL076502.

Ohfuchi, W., Nakamura, H., Yoshioka, M.K., Enomoto, T., Takaya, K., Peng, X., Yamane, S., Nishimura, T., Kurihara, Y. and Ninomiya, K. (2004) 10-km mesh meso-scale resolving global simulations of the atmosphere on the Earth Simulator-Preliminary outcomes of AFES (AGCM for the Earth simulator). *Journal of the Earth Simulator*, 1, 8–34.

Ou, N., Lin, Y. and Bi, X. (2015) Simulated heat sink in the Southern Ocean and its contribution to the recent hiatus decade. *Atmospheric and Oceanic Science Letters*, 8, 174–178.

Outten, S.D. and Esau, I. (2012) A link between Arctic sea ice and recent cooling trends over Eurasia. *Climatic Change*, 110, 1069–1075.

Reynolds, R.W., Smith, T.M., Liu, C., Chelton, D.B., Casey, K.S. and Schlax, M.G. (2007) Daily high-resolution-blended analyses for sea surface temperature. *Journal of Climate*, 20, 5473–5496.

Rogers, J.C. (1981) The North Pacific Oscillation. *International Journal of Climatology*, 1, 39–57.

Santer, B.D., Bonfils, C., Painter, J.F., Zelinka, M.D., Mears, C., Solomon, S., Schmidt, G.A., Fyfe, J.C., Cole, J.N.S. and Nazarenko, L. (2014) Volcanic contribution to decadal changes in tropospheric temperature. *Nature Geoscience*, 7, 185–189.

Screen, J.A., Deser, C. and Simmonds, I. (2012) Local and remote controls on observed Arctic warming. *Geophysical Research Letters*, 39, L10709.

Screen, J.A., Simmonds, I., Deser, C. and Tomas, R. (2013) The atmospheric response to three decades of observed Arctic sea ice loss. *Journal of Climate*, 26, 1230–1248.

Sun, L., Perlwitz, J. and Hoerling, M. (2016) What caused the recent "warm Arctic, cold continents" trend pattern in winter temperatures? *Geophysical Research Letters*, 43, 5345–5352.

Sung, M.K., Jang, H.Y., Kim, B.M., Yeh, S.W., Choi, Y.S. and Yoo, C. (2019) Tropical influence on the North Pacific Oscillation drives winter extremes in North America. *Nature Climate Change*, 9, 413–418.

Sung, M.K., Kim, B.M., Baek, E.H., Lim, Y.K. and Kim, S.J. (2016) Arctic-North Pacific coupled impacts on the late autumn cold in North America. *Environmental Research Letters*, 11, 084016.

Trenberth, K.E., Fasullo, J.T., Branstator, G. and Phillips, A.S. (2014) Seasonal aspects of the recent pause in surface warming. *Nature Climate Change*, 4, 911–916.

Wallace, J.M. and Gutzler, D.S. (1981) Teleconnections in the geopotential height field during the Northern Hemisphere winter. *Monthly Weather Review*, 109, 784–812.

Wang, H., Chen, H. and Liu, J. (2015) Arctic sea ice decline intensified haze pollution in eastern China. *Atmospheric and Oceanic Science Letters*, 8, 1–9.

Wang, S. and Liu, J. (2016) Delving into the relationship between autumn Arctic sea ice and central–eastern Eurasian winter climate. *Atmospheric and Oceanic Science Letters*, 9, 366–374.

Wang, T. and Miao, J. (2018) Twentieth-century Pacific Decadal Oscillation simulated by CMIP5 coupled models. *Atmospheric and Oceanic Science Letters*, 11, 94–101.

Watanabe, M., Shiogama, H., Tatebe, H., Hayashi, M., Ishii, M. and Kimoto, M. (2014) Contribution of natural decadal variability to global warming acceleration and hiatus. *Nature Climate Change*, 4, 893–897.

Xu, X., He, S., Gao, Y., Furevik, T., Wang, H., Li, F. and Ogawa, F. (2019) Strengthened linkage between midlatitudes and Arctic in boreal winter. *Climate Dynamics*, 53, 3971–3983.

Xu, X., He, S., Li, F. and Wang, H. (2018a) Impact of northern Eurasian snow cover in autumn on the warm Arctic–cold Eurasia pattern during the following January and its linkage to stationary planetary waves. *Climate Dynamics*, 50, 1993–2006.

Xu, X., Li, F., He, S. and Wang, H. (2018b) Sub-seasonal reversal of East Asian surface temperature variability in winter 2014/2015. *Advances in Atmospheric Sciences*, 35, 737–752.

Yeo, S.R., Kim, K.Y., Yeh, S.W., Kim, B.M., Shim, T. and Jhun, J.G. (2014) Recent climate variation in the Bering and Chukchi Seas and its linkages to large-scale circulation in the Pacific. *Climate Dynamics*, 42, 2423–2437.

Zhu, Y., Wang, H., Wang, T. and Guo, D. (2018) Extreme spring cold spells in North China during 1961–2014 and the evolving processed. *Atmospheric and Oceanic Science Letters*, 11, 432–437.

**How to cite this article:** Xu X, He S, Furevik T, *et al.* Oceanic forcing of the global warming slowdown in multi-model simulations. *Int J Climatol*. 2020;1–14. https://doi.org/10.1002/joc.6548